A R C H I V E O F M E C H A N I C A L E N G I N E E R I N G

VOL. LXI 2014 Number 4

10.2478/meceng-2014-0031

**Key words:** friction stir processing, aluminum alloy, response surface methodology

*MAREK STANISŁAW WĘGLOWSKI* *

# EXPERIMENTAL STUDY AND RESPONSE SURFACE METHODOLOGY FOR INVESTIGATION OF FSP PROCESS

The article presents the effect of rotational and travelling speed and down force on the spindle torque acting on the tool in Friction Stir Processing (FSP) process. The response surface methodology (RSM) was applied to find a dependence combining the spindle torque acting on the tool with the rotational speed, travelling speed and the down force. The linear and quadratic models with interaction between parameters were used. A better fitting was achieved for a quadratic model. The studies have shown that the increase in rotational speed causes a decrease in the torque while the increase in travelling speed and down force causes an increase in the torque. The tests were conducted on casting aluminium alloy AlSi9Mg. Metallography examination has revealed that the application of FSP process results in a decrease in the porosity in the modified material and microstructure refining in the stir zone. The segregation of Si and Fe elements was evident in the parent material, while in the friction stir processed area this distribution was significantly uniform.

## 1. Introduction

Various modification techniques have been developed to refine the microstructure of cast Al-Si alloys in recent years. The first category of methods is aimed at modifying the morphology of Si particles. Generally, chemical modification and thermal treatment have been adopted to modify the coarse acicular Si particles to fine and globular particles. The second research category refines the coarse primary aluminum phases. Heat treatment at an extremely high temperature for a short time results in a substantial refinement in the aluminum dendrites in a semisolid processed Al-Si alloys. These modification and heat-treatment techniques mentioned previously, unfortunately, cannot effectively eliminate the porosity in Al-Si, and redistribute the

* *Department of the Testing of Materials Weldability and Welded Construction, Institute of Welding, Bl. Czeslawa Str. 16-18, Gliwice 44-100, Poland; E-mail: marek.weglowski@is.gliwice.pl*

Si particles uniformly into the aluminum matrix. Therefore, a more effective modification technique is highly desirable for microstructural modification of cast aluminium alloy, such as Friction Stir Processing which was developed basing on friction stir welding (FSW) [1].

The FSP technique can be simply explained. A cylindrical, nonconsumable rotating tool made of high speed steel having a shoulder and pin is forced into the surface of the modified material. The pin penetrates the material until the tool shoulder reaches the surface and then, after obtaining the proper temperature, the movement of the tool or working table is started along a designed path on the material. The heat generated in the modified material is mainly caused by friction phenomena between the material and the surface of the tool and the portions of the stirring material [2]. A detailed description of the FSP process was presented in the previous papers [3].

In the last years, several investigations have been presented in the literature on some fundamentals of FSP and its process mechanics: for instance the microstructural evaluation occurring in the material [1, 4], physical concept of process [5, 6], and the occurring material flow [7, 8]. A wide research activity has been also focused on mechanical properties of the modified material [9]. Many different methods can be used to analyse the FSP process. Among other experimental techniques [5], analytical modelling [6], finite element analysis [10] and neural network techniques [11] are applied. One of the most interesting ways is to use the response surface methodology [11].

The goal of the presented work is to estimate the relationship between FSP parameters such as rotational and travelling speed, down force, and spindle torque. The experimental results are compared with results obtained from the response surface methodology.

## 2. Experiment

### 2.1. Course of the experiment

The FSP was conducted on a welding machine built on the base of a conventional vertical milling machine (Fig. 1). The machine was equipped with an appropriate device for measuring torque and forces (down force and travelling force). The mean value of the spindle torque was measured by the LOWSTIR head and calculated from 100 points in the area of the fully stabilized FSP process (Fig. 2).

The cylindrical FSP tool was made of HS6-5-2 high speed steel. The tool was machined to have a shoulder diameter of 22 mm, pin diameter 8 mm, and pin depth 4.5 mm. In addition, the pin had a spiral groove. The roughness

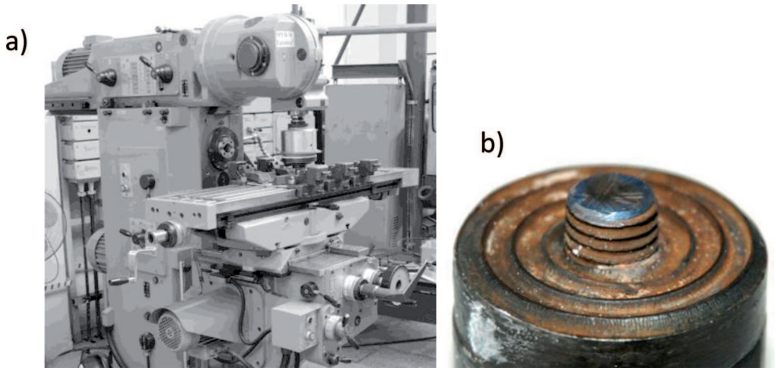


Fig. 1. Experimental setup a) general view, b) Friction Stir Processing tool

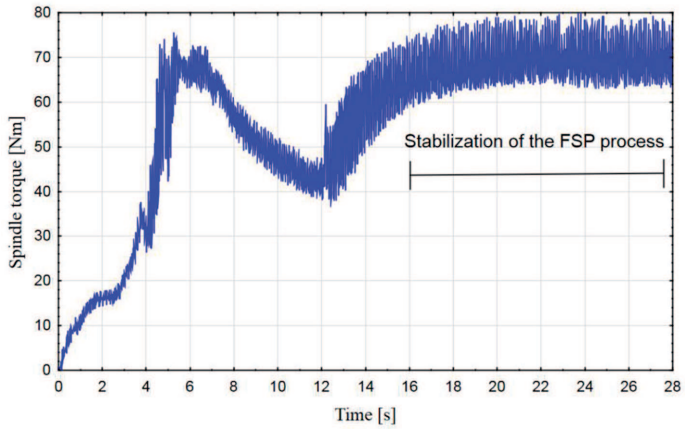


Fig. 2. Spindle torque signal recorded during FSP ($\omega$ = 560 rpm, $v$ = 710 mm/min)

and surface quality of test plates were like after milling. The plates were not cleaned.

To control the quality of the modified surface, the direct visual testing was carried out. The microstructure of the as-received and processed material was characterized by light (LM, NIKON MA200) and scanning (SEM, FEI Inspect S50 supplemented by energy dispersive spectrometry (EDS) provided by the EDAX company) microscopies. The samples were mechanically grounded followed by polishing with diamond paste. The final polishing was accomplished using $Al_2O_3$ suspension of about 0.25 μm. The observation was carried out without etching. The distribution of Mg, Al, Si, Fe was tested in the parent and modified material at the following parameters: numbers of frames 2048, resolution 256×256.

The workpiece was clamped tightly to an 8 mm thick plate made of plain carbon steel which served as a reinforcement, and then fixed to the machine table.

## 2.2. Identifying the range of parameters

The literature and the previous work done by the author have revealed that many independently controllable primary and secondary process parameters (as shown in Fig. 3) affect the torque acting on the tool. The primary process parameters such as rotational speed, travelling speed and down force were selected as process parameters for this study.

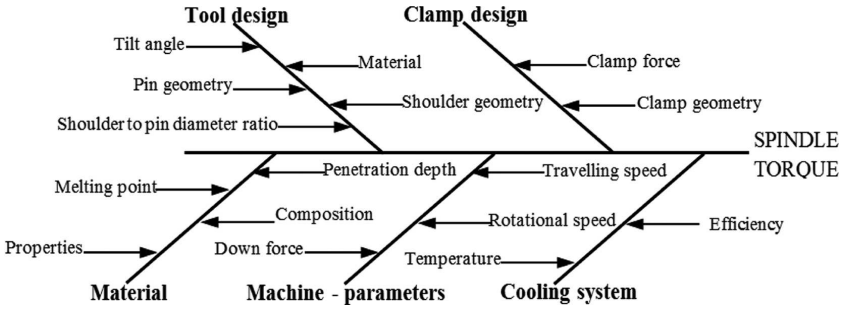


Fig. 3. Cause and effect diagram of factors influence on spindle torque during FSP

In the present investigation, a cast AlSi9Mg material was processed using 27 different combination of tool rotation and travelling speed, as summarized in Fig. 4. The maximum travelling speed of the milling machine was 1120 mm/min. The minimum speed below 112 mm/min was too low due to the efficiency of FSP process. Each of these processes involved a traverse approximately 180 mm in length. The tool tilt angle was kept constant at 1.5°.

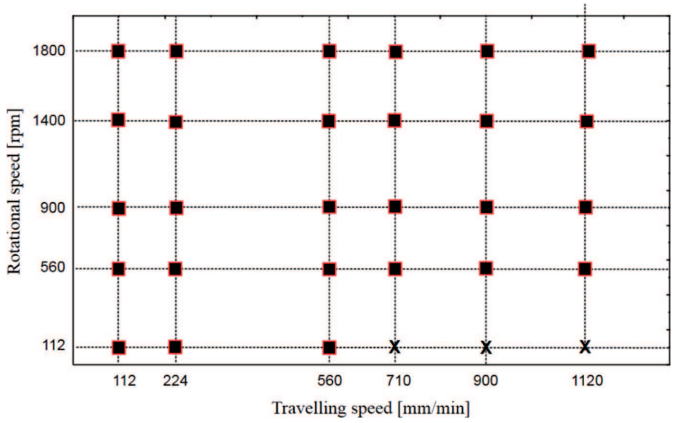


Fig. 4. The area of technological parameters of FSP, ■ – experimental parameters, × – the parameters are out of the range of maximum power of the FSW machine

### 2.3. Response surface methodology

The practical application of the response surface methodology (RSM) requires developing an approximating model for the true response surface. The underlying true response surface is typically driven by some unknown physical mechanism – friction stir processing. The approximating model is based on the observed data from the experiment, and is a collection of the empirical models. Multiple regression is a collection of statistical techniques useful for building the types of empirical models required in RSM [12].

In general, the response variable $y$ may be related to $k$ independent variables. The model

$$y = b_0 + b_1x_1 + b_2x_2 + b_3x_3 + \ldots + b_kx_k + \varepsilon \tag{1}$$

is called a multiple linear regression model with k independent variables. The parameters $b_j$, $j = 0, 1, 2, 3 \ldots, k$, are the regression coefficients. The residual $\varepsilon$ is a term that represents other sources of variability. Thus $\varepsilon$ incudes effects such as measurement error on the response, other sources of variation that are inherent in the process (background noise) and the effect of other (possible unknown) variables. This model describes a hyperplane in the k-dimensional space of the independent variables $\{x_j\}$. The parameter $b_j$ represents the expected change in response $y$ per unit change in $x_j$ when all the remaining independent variables $x_i$ $(i \neq j)$ are held constant.

The paper presents the development of the empirical model relating the torque acting on the tool and the rotational speed, travelling speed and down force. A first order response surface model that might describe this relationship is as follows:

$$y = b_0 + b_1x_1 + b_2x_2 + b_3x_3 + \varepsilon \tag{2}$$

where $y$ represents the torque acting on the tool, $x_1$ represents the rotational speed, $x_2$ represents the travelling speed and $x_3$ represents the down force. This model is a multiple linear regression model with three independent variables. The model describes a plane in the three-dimensional $x_1$, $x_2$ and $x_3$ space. The parameter $b_0$ fixes the intercept of the plane.

A more complex model, in which interaction terms are taken into account, can be written as:

$$y = b_0 + b_1x_1 + b_2x_2 + b_3x_3 + b_4x_1x_2 + b_5x_1x_3 + b_6x_2x_3 + \varepsilon \tag{3}$$

The most complex model, taking into account interaction between independent variables and squares of the variables, is the second-order response surface model:

$$y = b_0+b_1x_1+b_2x_2+b_3x_3+b_4x_1x_2+b_5x_1x_3+b_6x_2x_3+b_7x_1^2+b_8x_2^2+b_9x_3^2+\varepsilon \tag{4}$$

In the presented investigation these models were used for prediction of the value of torque acting on the tool. The modeling was performed using the STATISTICA platform version 10, module Design of Experiments (DOE).

## 3. Results and discussion

The influence of the rotational speed on the torque acting on the tool is shown in Fig. 5. The increase of this speed causes a decrease in the value of torque. This is due to the fact that the increase in rotational speed of the tool causes an increase in temperature in the stir zone. Hence, the friction coefficient becomes lower and therefore the resistance of the modified material decreases. At the same time, the tendency of the material to plastic deformation is higher. The numerical modeling of these phenomena [7] revealed that two zones occurred in the friction stir area, that is a primary and a secondary zone. As the tool rotation speed increases, the diameter of the primary zone vortex decreases, and the process zone, itself, shows less tilt. With the increasing tool rotation speed, the concentration of streamlines within the secondary process zone also increases, indicating an increase in the coherency of this zone at the trailing edge of the tool.

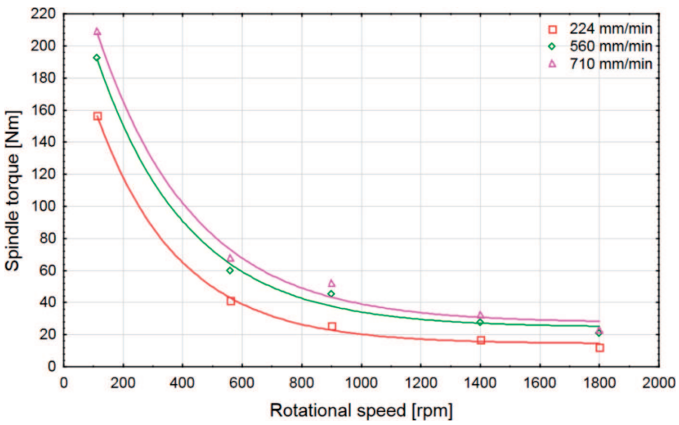


Fig. 5. Influence the rotational speed on the torque acting on the tool

On the other hand, the spindle torque is not significantly affected by the change in the travelling speed (Fig. 6). The decrease in torque with the decreasing travelling speed at constant rotational speed [13] may be due to two contributing factors. Firstly, for a constant tool rotation speed and decreasing travelling speed, the volume of material being deformed on each revolution decreases, hence the heat is generated in a smaller volume, and this in turn may lead to slightly higher temperatures and lower flow stress. Secondly, lower travelling speed will reduce the convective cooling, resulting

from slower movement into the relatively cooler material in the front of the tool. The previous numerical modelling of the FSP process revealed [7] that, when the tool velocity increases, the primary process zone remains well developed, but the streamlines begin to "lag behind" the advancing tool causing the vortex to tilt from the leading edge toward the trailing edge into the workpiece thickness. At the same time, the diameter of the vortex has increased, indicating a loss in its degree of coherency. The secondary zone also remains clearly defined; however, the size of the secondary zone has decreased.

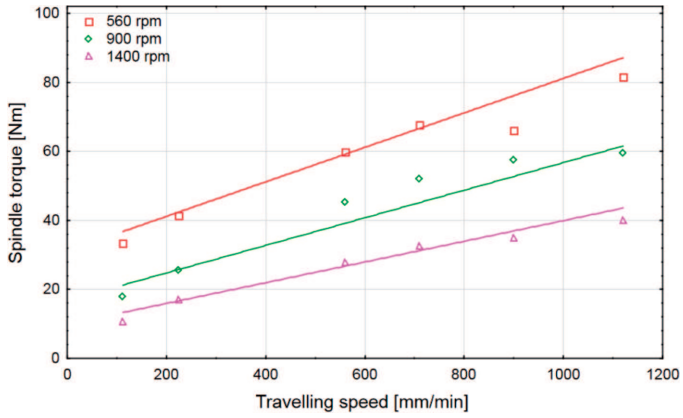


Fig. 6. Influence of the travelling speed on the torque acting on the tool

During the experiments, the penetration depth was kept constant (control by the machine operator). Hence, the value of the down force depends on rotational and travelling speed and also machine operator. The influence of the down force on spindle torque is shown in Fig. 7. It is evident that the increase of down force causes the increase in the torque.

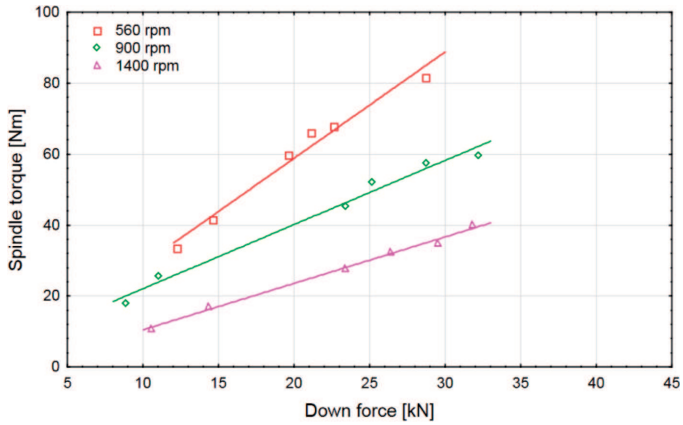


Fig. 7. Influence of the down force on the torque acting on the tool

As mentioned before the value of spindle torque is influenced by rotational speed, travelling speed, down force, type and shape of the tool, and the kind of modified material. The response surface methodology (RSM) has been applied in order to find a dependence combining the torque acting on the tool with the rotational speed in a wider range (112÷1800 rpm), the travelling speed in the range of 112÷1120 mm/min and down force. RSM has been built in Statistica software. Rotational and travelling speeds and down force were introduced as independent variables. A first order and second-order response surface models were used during mathematical modeling. The interactions between the independent variables were assumed in the model.

In the first step, in order to determine the relationship between parameters and torque based on RSM, a linear model was assumed. Equation (3) may be presented as:

$$M = B_0 + B_1\omega + B_2 v + B_3 F_d + B_4\omega v + B_5\omega F_d + B_6 v F_d \tag{5}$$

The calculation results of the regression coefficients for the linear model are shown in Table 1. The calculation results indicate the significance level p where linear main effects are statistically significant ($p < 0.05$), suggesting that a linear model containing the interaction is sufficient.

Table 1.
Results of calculation of regression coefficients for linear model (rounding of the number)

| The regression coefficients | Values | Probability – p |
|---|---|---|
| B0 | – 13.3548 | 0.0 |
| B1 | – 0.0019 | 0.0 |
| B2 | – 0.0428 | 0.004778 |
| B3 | 6.6789 | 0.000094 |
| B4 | 0.0000 | 0.017894 |
| B5 | – 0.0031 | 0.001727 |
| B6 | – 0.0013 | 0.010626 |

The Pareto chart of effects was used for communicating the results of an experiment (Fig. 8). In this graph, the ANOVA effect estimates were sorted from the largest absolute value to the smallest absolute value. The magnitude of each effect is represented by a column, and a line going across the columns indicates how large an effect has to be (i.e., how long a column must be) to be statistically significant. From Fig. 8 one can clearly observe that the most significant effect on torque is that of the rotational speed. In turn, the lowest impact has the interaction between rotational speed and traveling speed.

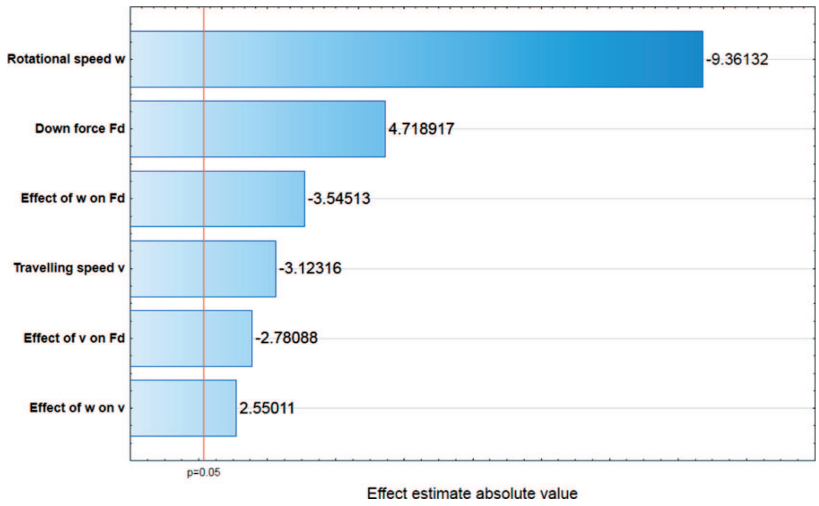


Fig. 8. The Pareto chart of effects for linear model

A quadratic model was assumed in the second step while determining the relationship between parameters and torque based on RSM. Equation (4) may be presented as:

$$M = B_0 + B_1\omega + B_2 v + B_3 F_d + B_4 \omega v + B_5 \omega F_d + B_6 v F_d + B_7 \omega^2 + B_8 v^2 + B_9 F_d^2 \quad (6)$$

The calculation results of the regression coefficients for the model, taking into account the interactions between independent values, are given in Table 2.

Table 2.
Results of calculation of regression coefficients for quadratic model with interaction (rounding of the number)

| The regression coefficients | Values | Probability – p |
|---|---|---|
| $B_0$ | 27.01169 | 0.0 |
| $B_1$ | – 0.05624 | 0.0 |
| $B_2$ | – 0.00224 | 0.030708 |
| $B_3$ | 4.10589 | 0.001253 |
| $B_4$ | 0.00003 | 0.004113 |
| $B_5$ | – 0.00241 | 0.000922 |
| $B_6$ | – 0.00527 | 0.024594 |
| $B_7$ | 0.00002 | 0.003173 |
| $B_8$ | 0.00007 | 0.021726 |
| $B_9$ | 0.06837 | 0.082440 |

The linear effects and interactions are statistically significant ($p < 0.05$), while the quadratic parameter $B_9$ at the down force is statistically insignificant ($p > 0.05$).

The Pareto chart of effects for quadratic model is shown in Fig. 9. According to Fig. 9, it is clear that the rotational speed has the most significant effect on torque. In turn, traveling speed has the lowest impact.

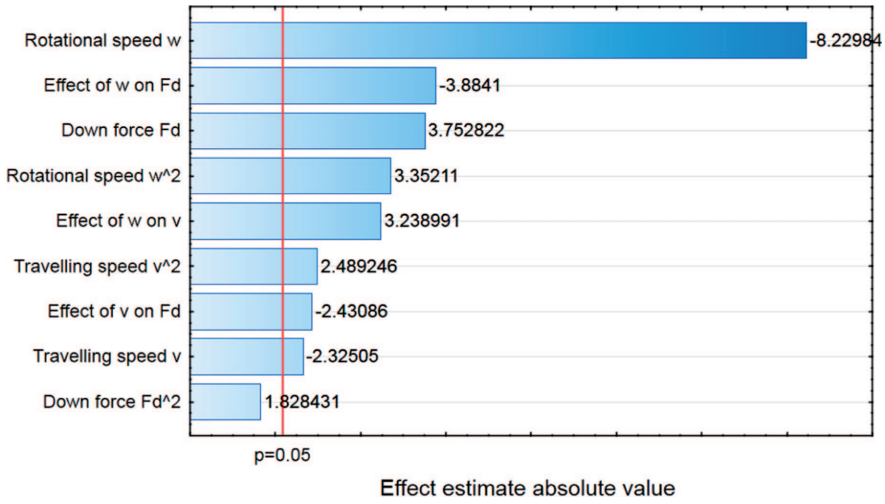


Fig. 9. The Pareto chart of effects for quadratic model

The comparison of results obtained from the experiments, the linear model and quadratic model are shown in Fig. 10. The results indicate that better fitting was achieved for quadratic model $R^2 = 0.99763$ (for linear model $R^2 = 0.98924$). Based on the achieved results, the quadratic model can be recommended for predicting the value of spindle torque acting on the tool during FSP process being carried out on cast aluminium alloy AlSi9Mg.

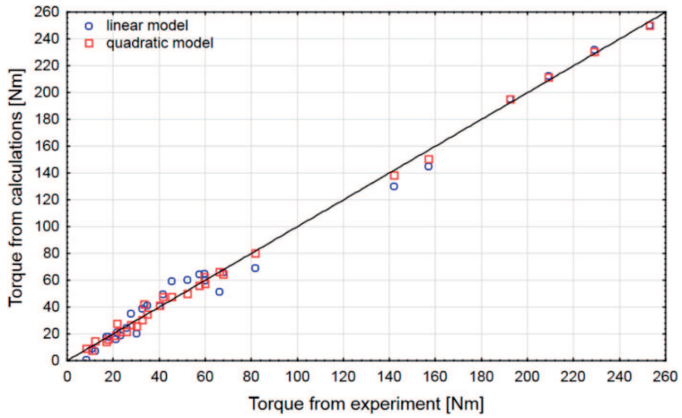


Fig. 10. Comparison between experimental results and calculations

## 4. Microstructural characterization

The typical LM microstructure of the processed material is shown in Fig. 11. Two well-defined regions could be easily distinguished: the parent material (Fig. 12) and the FSP area (in the dashed line area Fig. 11). The parent material was characterized by the coarse grained structure with pores, while the microstructure in the processed zone was modified by the tool action. The result of modification in the processed area was refinement of the microstructure. Further, the porosity in the as cast AlSi9Mg sample was nearly eliminated by FSP. The principal microstructural components of this alloys in as-cast state are (Al) dendrites and (Al)+(Si) eutectic. The light and scanning electron microscopy examination revealed characteristic dendrites in the base material (Fig. 12). In the FSP area (Fig. 13), the broken Si particles have a size ranging from submicron to more than ten micrometers. The segregation of Si and Fe elements was evident in the parent material (Fig. 14). The distribution of Si and Fe particles in the friction stir processed area was significantly improved compared to that in the as-cast sample (Fig. 15). This is caused by the action of the rotating tool.

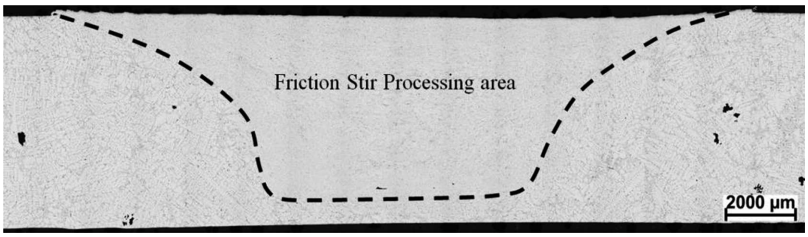


Fig. 11. Typical cross-section of the processed surface area; light microscope, ($\omega$ = 560 rpm, $v$ = 560 mm/min)

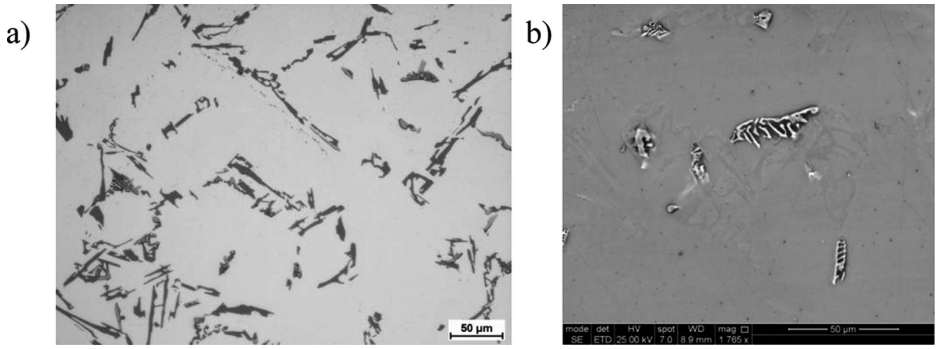


Fig. 12. Micrograph of parent material, a) light microscope, b) SEM

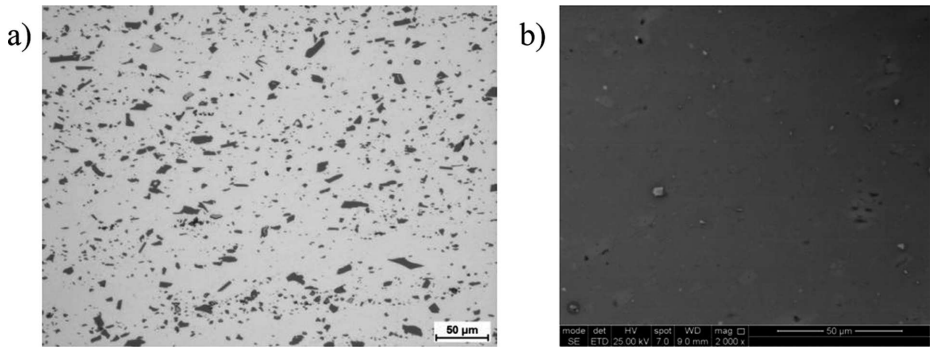


Fig. 13. Micrograph of modified surface, ($\omega$ = 560 rpm, $v$ = 560 mm/min), a) light microscope, b) SEM

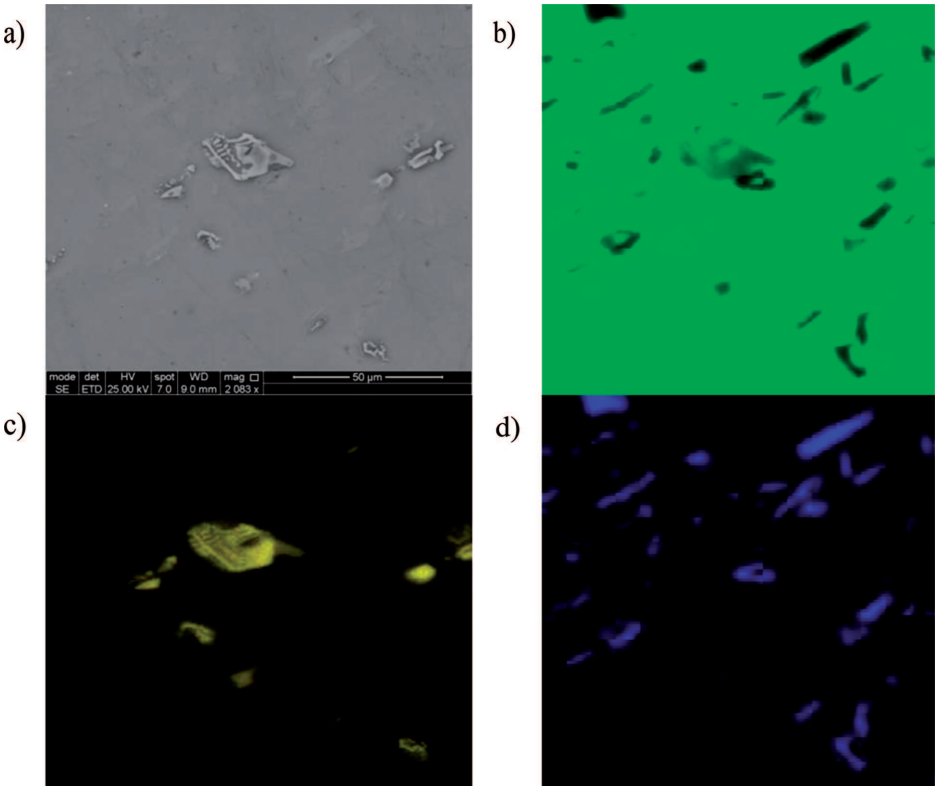


Fig. 14. Distribution map of the elements in parent material, a) SEM micrograph, b) Al, c) Fe, d) Si

## 5. Conclusions

The present study has examined the relationship between parameters of FSP process and spindle torque, and microstructure of a modified AlSi9Mg alloy. The conclusions are as follows:

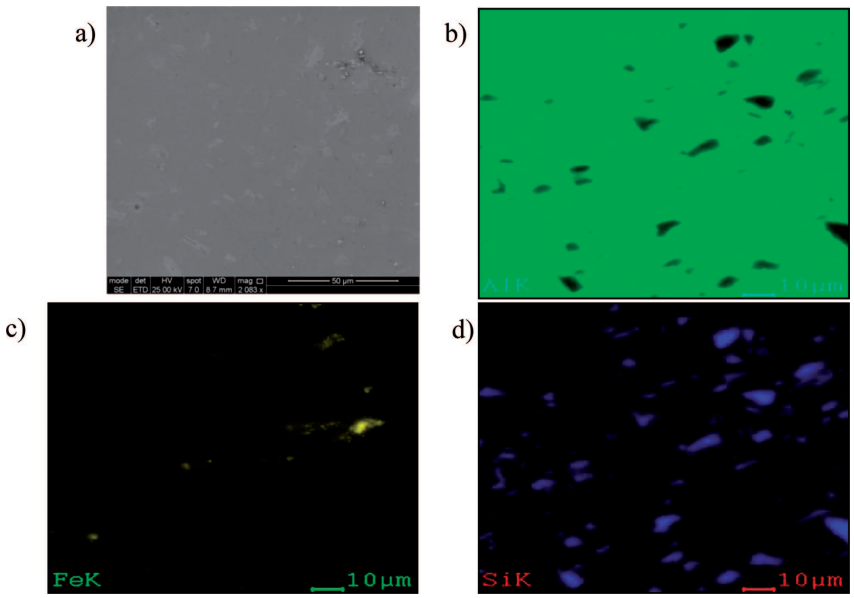


Fig. 15. Distribution map of the elements in the modified material, ($\omega$ = 560 rpm, $v$ = 560 mm/min), a) SEM micrograph, b) Al, c) Fe, d) Si

- the increase in the rotational speed decreases the torque acting on the tool,
- the increase in the travelling speed and down force increases the torque acting on the tool,
- the surface response methodology is a useful technique to determine the impact of the parameters of the process on the spindle torque. In this study, a square model with interaction assured the better fitting,
- FSP resulted in the significant breakup of Si particles and aluminum dendrites, and in the modified material amore uniform distribution of Si and Fe was obtained.

## Acknowledgements

This work was performed with funding from Polish Ministry of Science and Higher Education as a part of statutory activity of Instytut Spawalnictwa (Institute of Welding).The author would like to express his appreciation to Professor Stanislaw Dymek and Izabela Kalemba Ph.D. from the Department of Surface Engineering & Materials Characterisation at the AGH University for their support during the course of this research.

Manuscript received by Editorial Board, February 23, 2014;
final version, August 13, 2014.

REFERENCES

[1] Ma Z.Y., Sharma S.R., Mishra R.S.: Microstructural Modification of As-Cast Al-Si-Mg Alloy by Friction Stir Processing. Metallurgical and Materials Transactions A: Physical Metallurgy and Materials Science 37 (2006) 3323-3336.
[2] Oh-Ishi K., McNelley T.R.: The Influence of Friction Stir Processing Parameters on Microstructure of As-Cast NiAl Bronze. Metallurgical and Materials Transactions A: Physical Metallurgy and Materials Science 36 (2005) 1575-1585.
[3] Węglowski M.St.: Technologia Friction Stir Processing – nowe możliwości. Biuletyn Instytutu Spawalnictwa 55 (2011) 25-31.
[4] Węglowski M.St., Dymek S.: Microstructural modification of cast aluminium alloy AlSi9Mg via Friction Modified Processing. Archives of Metallurgy and Materials 57 (2012) 71-78.
[5] Węglowski M.St., Pietras A.: Friction Stir Processing – analysis of the process. Archives of Metallurgy and Materials 56 (2011) 779-788.
[6] Schmidt H., Hattel J., Wert J.: An analytical model for the heat generation in friction stir welding. Modeling and Simulation in Materials Science and Engineering 12 (2004) 143-157.
[7] Węglowski M.St., Hamilton C., Dymek S.: A coupled thermal/material flow model of friction stir surfacing applied to AlMg9Si. Materials Engineering 34 (2013) 201-204.
[8] Cui G.R., Ma Z.Y., Li S.X.: Periodical plastic flow pattern in friction stir processed Al-Mg alloy. Scripta Materialia 58 (2008) 1082-1085.
[9] Kopuściański M., Węglowski M.St., Pietras A., Węglowska A., Hamilton C., Dymek S.: Friction Stir processing as a fabricating route of dispersion strengthened aluminum alloys. Materials Engineering 34 (2013) 303-305.
[10] Paradiso V., Astarita A., Carrino L. et al.: Numerical optimization of selective superplastic forming of friction stir processed AZ31 Mg alloy. Key Engineering Materials 554-557 (2013) 2212-2220.
[11] Lakshminarayanan A.K., Balasubramanian V.: Comparison of RSM with ANN in predicting tensile strength of friction stir welded AA7039 aluminium alloy joints. Trans. Nonferrous Met. Soc. China 19 (2009) 9-18.
[12] Myers R.H., Montgomery D.C., Anderson-Cook Ch.M.: Response Surface Methodology. Process and product optimization using design experiments. New York, Wiley, 2009.
[13] Arora A., Nandan R., Reynolds A.P., DebRoy T.: Torque, power requirement and stir zone geometry in friction stir welding through modelling and experiments. Scripta Materialia 60 (2009) 13-16.

**Badanie procesu FSP poprzez badania doświadczalne i metodę powierzchni odpowiedzi**

Streszczenie

W pracy przedstawiono wpływ prędkości obrotowej i przesuwu narzędzia oraz siły docisku na moment obrotowy działający na narzędzia w procesie tarciowej modyfikacji z mieszaniem materiału (FSP). Do wyznaczenia zależności pomiędzy momentem a prędkościami obrotową i przesuwu oraz siłą docisku wykorzystano metodę powierzchni odpowiedzi. Wykorzystano modele liniowy i kwadratowy uwzględniające interakcje pomiędzy parametrami wejściowymi. Lepsze dopasowanie zapewnił model kwadratowy. Wyniki badań wykazały, iż wzrost prędkości obrotowej narzędzia powoduje zmniejszenie momentu działającego na narzędzie, natomiast wzrost prędkości przesuwu i siły docisku powoduje wzrost momentu. Badania były przeprowadzone na odlewniczym stopie aluminium AlSi9Mg. Badania metalograficzne ujawniły, że zastosowanie procesu FSP powoduje rozdrobnienie ziarna oraz redukcję porowatości w obszarze mieszania. Wyraźna segregacja Si i Fe w materiale rodzimym została wyeliminowana, a rozkład pierwiastków jest bardziej jednorodny.